2011 International Nuclear Atlantic Conference - INAC 2011
Belo Horizonte,MG, Brazil, October 24-28, 2011
ASSOCIAÇÃO BRASILEIRA DE ENERGIA NUCLEAR - ABEN
ISBN: **978-85-99141-04-5**

NEUTRON ACTIVATION OF MICROSPHERES CONTAINING ^{165}Ho: THEORETICAL AND EXPERIMENTAL RADIONUCLIDIC IMPURITIES STUDY

Peterson L. Squair, Lorena Pozzo, Evandro Ivanov and João A. Osso Jr.

Instituto de Pesquisas Energéticas e Nucleares (IPEN / CNEN - SP)
Diretoria de Radiofarmácia (DIRF)
Gerência de Pesquisa, Desenvolvimento e Inovação (GPD)
Av. Professor Lineu Prestes 2242
05508-000 São Paulo, SP
peterson.squair@ipen.br

ABSTRACT

The ^{166}Ho microspheres are potentially interesting for medical applications for treatment of many tumors. The internal radionuclide therapy can use polymer or glass device that provides structural support for the radionuclide. After activation, beta minus emission of ^{166}Ho ($T_{1/2}$=26.8h, β^- E_{max}=1.84 MeV, γ E_p=80.6 keV) can be used for therapeutic purposes. The aim of this work is study the influence of radionuclide impurities between End of Bombardment (EOB) and the medical application. The appropriate specific activities and purity along decay should be adequate for their safe and efficient medical applications. The good practices on neutron activation techniques are choice a high purity target to avoid production of undesirable radionuclides and when possible with enriched targets to obtain higher specific activity. In this work the target used was Ho_2O_3 and polymeric microspheres containing holmium acetylacetonate (HoAcAc) manufactured at the Biotechnology Center-IPEN/CNEN-SP. Three conditions were evaluated: preliminary test with $1.0x10^{13}n.cm^{-2}s^{-1}$ for 1.0 hour; nowadays maximum capability of IEA-R1 reactor with $5.0x10^{13}n.cm^{-2}s^{-1}$ for 64.0 hours and the ideal IEA-R1 operation with $5.0x10^{13}n.cm^{-2}s^{-1}$ for 120.0 hours. Considering the sample with 99.9% ^{165}Ho purity and 0.1% for each impurities elements with its natural abundance, the highest radionuclidic impurity is the Lutetium followed by Ytterbium, Lanthanum and Cerium. The intrinsic radionuclidic impurity of ^{166m}Ho is less relevant. This review is important to identify the radionuclidic purity characteristics of the preliminary studies with different time and flux irradiation. The data produced in this paper will help to define strategies for the production of ^{166}Ho radioisotope at IEA-R1 IPEN/CNEN-SP reactor.

1. INTRODUCTION

Liver cancer is not among the most prevalent cancer in Brazil. However, high technology is required for its proficient diagnosis and treatment. According to the consolidated data on cancer mortality in Brazil, this disease is not in the top ten incidents with incidence rate between 1.07 to 9.34/100,000 for men and 0.28 to 7.04/100,000 for women [1]. Therefore, liver metastases frequently occur during the progression of various solid tumors, especially colorectal cancers with 14/100,000 incidence rate for women and 15/100,000 for men [2,3,4].

One type of therapy of this disease can be an alternative radiotherapy mode with the use of radioactive microspheres injection in liver's artery with a diameter between 20 and 50 µm. The basis for such therapy is that tumors are usually rich in vasculature and that liver metastases are almost exclusively dependent on arterial blood supply [5]. Microspheres are characterized by high specific uptake in organs and tissues, this process can be controlled by variation of physico-chemical properties of microparticles and by varying procedures of

administration [6]. Poly-L-lactic acid is the optimal polymer for preparing microspheres; its density is close to that of blood and it can be metabolized in the living body. Microspheres of poly-L-lactic acid labeled with ^{166}Ho can be obtained by incorporation of stable ^{165}Ho in the particles and by subsequent irradiation with thermal neutrons [6]. The polymeric microspheres labeled with ^{165}Ho, manufactured at the Biotechnology Center-IPEN/CNEN-SP with size raging between 20 to 50 µm also gave good results on the fabrication process [7].

The potential use of polymeric microspheres labeled with ^{165}Ho combines low density, biocompatibility microspheres and immobilization of ^{166}Ho, which has favorable physical characteristics for image guided radionuclide therapy [8]. The ^{166}Ho decay by beta emission ($T_{1/2}$=26.8h, E_{max}=1.84 MeV) for therapeutic purposes and gama emission (80.6 keV – 6.7%) that can be used for image produce. This photon allows dosimetric calculations during administration, and contributes to only 1.1% of the overall absorbed radiation dose [9]. Dosimetric studies can give an idea of the potential efficacy of treatments [10].

The ^{166}Ho is produced by exposing suitable target materials containing ^{165}Ho to the neutron flux in a nuclear reactor for an appropriate time to occur the (n,γ) reaction. The ^{165}Ho has a natural abundance of 100% and a cross-section of 64 b to produce ^{166}Ho, allowing short neutron activation times [11]. However, during the ^{165}Ho activation process the ^{166m}Ho ($T_{1/2}$=1200y, 3.1 barn) will always be produced, but with a lesser yield and others elements present on the target will be activated. Target purity is important to avoid radionuclidic impurities after irradiation. The possible contaminants of holmium targets are rare earths such as Ytterbium, Lutetium, Lanthanum and Cerium [12]. The radionuclidic impurities level depends on the irradiation characteristics at the nuclear reactor.

The irradiation process can change the polymeric microsphere structure. This event was observed by Nijsen during neutron activation of the polymeric microspheres (Ho-PLA) that neutron flux at $5x10^{13}$ $cm^{-2}.s^{-1}$ for more than 1 h [13]. However, the radiation limits to produce changes at the microspheres are still indefinite. The irradiation parameters affecting the integrity to a greater or lesser extent were irradiation time, the facility, the amount of microspheres per vial, water content of the microspheres and material of the vial [13].

This study describes the radionuclidic impurity level for three theoretical and one experimental irradiation parameters: preliminary test with neutron flux at $1x10^{13}$ $cm^{-2}.s^{-1}$ for 1 h, IEA-R1 IPEN Reactor maximum nowadays capability with neutron flux at $5x10^{13}$ $cm^{-2}.s^{-1}$ for 64 h and with neutron flux at $5x10^{13}$ $cm^{-2}.s^{-1}$ for 120 h. The definition of irradiation conditions is necessary to reduce the unnecessary patient dose due to radionuclidic impurities and the optimization of these parameters result in a good practical method for the production of microspheres loaded with holmium. The structural changes on the microspheres after irradiation were not studied.

2. MATERIALS AND METHODS

2.1. Theoretical analyses

The theoretical activation was used to evaluate the possible contamination by four rare earth compounds considering their natural abundance. These rare earths were Ytterbium, Lutetium, Lanthanum and Cerium. The physical data used to calculate activities of the isotopes are shown in table 1. The analyses consider only the thermal neutron flux to determine the activities. The activity calculus is given by the expression:

$$A_0 = \frac{m \cdot \Theta}{A} \cdot N_A \cdot \sigma_\gamma \cdot \Phi_{th} \cdot \left(1 - e^{-\lambda \cdot t}\right) \cdot e^{-\lambda \cdot t_d} \qquad (01)$$

Where m is the mass of the element to be irradiated in grams, the factor Θ is isotopic abundance of target nucleus, A is the atomic mass of the element, N_A is the Avogadro's number, σ_γ is the neutron capture cross section of the target nucleus in cm², Φ_{th} is the thermal neutron flux, λ is the decay constant of the produced radionuclide, t is the time of irradiation in seconds and t_d is the decaying time after irradiation in seconds.

The activities of the radioisotopes were calculated for holmium at three irradiation conditions with neutron flux at $1x10^{13}$ $cm^{-2}.s^{-1}$ for 1 h, $5x10^{13}$ $cm^{-2}.s^{-1}$ for 64 h and $5x10^{13}$ $cm^{-2}.s^{-1}$ for 120 h, considering the 99.9% purity level of the holmium and 0.1% for each impurities at their natural abundances. In order to evaluate the level of radionuclidic impurities, their activities were calculated within EOB within 144 hours.

Table 1. Physical data of isotopes [14].

Element	Isotope	Atomic mass (g)	Isotopic compositions	Cross section (*b*)	Product (n,γ)	$T_{(1/2)}$
Holmium	Holmium-165	164.93	100.0%	64.7	Holmium-166	26.794 h
	Holmium-165	164.93	100.0%	3.1	Holmium-166m	1200 y
Ytterbium	Ytterbium-168	167.93	0.13%	2230.0	Ytterbium-169	32.026 d
	Ytterbium-174	173.94	31.83%	69.4	Ytterbium-175	4.185 d
Lutetium	Lutetium-175	174.94	97.41%	21.0	Lutetium-176m	3.635 h
	Lutetium-176	175.94	2.59%	2065.0	Lutetium-177	6.734 d
	Lutetium-176	175.94	2.59%	3.0	Lutetium-177m	160.4 d
Lanthanum	Lanthanum-139	138.91	99.90%	8.93	Lanthanum-140	1.6781 d
Cerium	Cerium-140	139.91	88.40%	0.57	Cerium-141	32.501 d
	Cerium-142	141.91	11.10%	0.95	Cerium-143	33.039 h

2.2. Experimental analyses

All irradiations were performed in the IEA-R1 reactor facilities at IPEN/CNEN-SP. The experimental activation process was performed with neutron flux of $1x10^{13}$ $cm^{-2}.s^{-1}$ for 1 h in "eppendorf" vials which were enclosed in sealed aluminum tube ("rabbits"). The samples masses were around 10 mg and the purity level of Holmium was unknown. The polymeric microspheres were manufactured by IPEN Biotechnology Center with PDLA, poly(D,L,lactic) containing holmium acetylacetonate complex (HoAcAc) and PLLA, poli(L,lactic) containing HoAcAc. Holmium Oxide (Ho_2O_3) with 99.9% purity level was used as reference to compare the theoretical and experimental results.

After irradiation process and an appropriate waiting time, the activities of ^{166}Ho and radionuclidic impurities were measured by using a γ-ray spectrometer. The γ-ray spectrometer was a high purity germanium detector (HPGe). The HPGe detector was coupled to a computer based multi-channel analyzer, which can integrate the photo peak area (net area) of γ-ray spectra. The energy and efficiency calibrations were performed with a set of standard sources such as ^{152}Eu, ^{137}Cs, ^{60}Co and ^{133}Ba. The two measuring times and appropriate distances between the sample and the surface detector were chosen based on the activity and the lower and higher half-life of each radioactive isotope. The dead times were below 10% for all measurements.

For evaluate the activities of the reaction products formed via n,γ reaction, it was chosen the γ-ray peaks with well separated and net area uncertainty lower than 30%. The γ-ray peaks analyses shown in table 2 and the activities value given by the expression:

$$A_{EOB} = \frac{C}{I \cdot Ef \cdot t \cdot e^{-\lambda \cdot (t_m - t_{EOB})}} \qquad (02)$$

Where A_{EOB} is the activity at End of Bombardment, C is the net area reported by software, I is the γ-ray peaks emission abundances, Ef is the detection efficiency, t is the counting time in seconds, λ is the decay constant, (t_m-t_{EOB}) express the time between End of Bombardment and measurements.

Table 2. Gamma energy and emission abundances [14].

Radioisotope	γ-ray Isotope					
	Energy (keV)	Intensity	Energy (keV)	Intensity	Energy (keV)	Intensity
Holmium-166	80.6	6.7 %	1379.4	0.93 %	1581.9	0.2 %
Holmium-166m	184.4	72.6 %	810.3	58.1 %	711.7	55.3 %
Ytterbium-169	63.1	44.2 %	197.9	35.8 %	177.2	22.2 %
Ytterbium-175	396.3	6.4 %	282.5	3.0 %	113.8	1.9 %
Lutetium-176m	88.3	8.9 %	---	---	---	---
Lutetium-177	208.4	11.0 %	112.9	6.4 %	321.3	0.2 %
Lutetium-177m	208.4	57.7 %	228.5	37.0 %	378.5	29.7 %
Lanthanum-140	1596.2	95.4 %	487.0	45.5 %	815.8	23.3 %
Cerium-141	145.4	48.2 %	---	---	---	---
Cerium-143	293.3	42.8 %	57.4	11.7 %	664.6	5.7 %

3. RESULTS AND DISCUSSION

3.1. Theoretical analyses

The theoretical specific activities have been calculated to ten radioisotopes at three irradiation conditions. The results are shown in table 3.

Table 3. Specific activities results by theoretical method.

Theoretical - Radionuclides Activity at EOB (Bq.g^{-1})									
^{166}Ho	^{166m}Ho	^{169}Yb	^{175}Yb	^{176m}Lu	^{177}Lu	^{177m}Lu	^{140}La	^{141}Ce	^{143}Ce
Neutron flux: 1.0x10^{13} n.cm^{-2}.s^{-1} Time: 1 h									
60.3E+9	7.5E+3	93.7E+6	5.3E+9	122.3E+9	7.8E+9	478.8E+3	6.6E+9	19.3E+6	92.9E+6
Neutron flux: 5.0x10^{13} n.cm^{-2}.s^{-1} Time: 64 h									
9.6E+12	2.4E+6	29.2E+9	1.4E+12	3.5E+12	2.2E+12	152.4E+6	1.3E+12	6.0E+9	16.5E+9
Neutron flux: 5.0x10^{13} n.cm^{-2}.s^{-1} Time: 120 h									
11.3E+12	4.5E+6	53.3E+9	2.2E+12	3.5E+12	3.7E+12	284.2E+6	1.7E+12	11.0E+9	20.6E+9

These results of specific activities are used to determine the radionuclidic impurity level for the 99.9% purity of holmium. The determination of impurity levels were established for the

three activation conditions from the EOB to the maximum decay time of 7 days and results shown in tables 4, 5 and 6 and figures 1, 2 and 3.

Table 4. Radionuclidic impurities level to preliminary test conditions.

	Radionuclidic Impurity Level (Flux 1x10^{13} n.cm^{-2}.s^{-1} at 1 h with 99.9%)									
ΔT	^{166m}Ho	^{169}Yb	^{175}Yb	^{176m}Lu	^{177}Lu	^{177m}Lu	^{140}La	^{141}Ce	^{143}Ce	Σ
EOB	1.2E-07	1.6E-06	8.8E-05	2.0E-03	1.3E-04	7.9E-09	1.1E-04	3.2E-07	1.5E-06	2.4E-03
24 h	2.3E-07	2.9E-06	1.4E-04	3.9E-05	2.2E-04	1.5E-08	1.3E-04	5.8E-07	1.7E-06	5.4E-04
48 h	4.3E-07	5.2E-06	2.2E-04	7.4E-07	3.6E-04	2.7E-08	1.7E-04	1.1E-06	2.0E-06	7.6E-04
72 h	8.0E-07	9.6E-06	3.4E-04	1.4E-08	6.1E-04	5.1E-08	2.0E-04	1.9E-06	2.2E-06	1.2E-03
96 h	1.5E-06	1.8E-05	5.4E-04	2.7E-10	1.0E-03	9.4E-08	2.5E-04	3.5E-06	2.5E-06	1.8E-03
120 h	2.8E-06	3.2E-05	8.6E-04	5.2E-12	1.7E-03	1.7E-07	3.1E-04	6.4E-06	2.8E-06	2.9E-03
144 h	5.2E-06	5.9E-05	1.4E-03	1.0E-13	2.9E-03	3.2E-07	3.8E-04	1.2E-05	3.1E-06	4.7E-03
168 h	9.6E-06	1.1E-04	2.1E-03	1.9E-15	4.9E-03	6.0E-07	4.7E-04	2.1E-05	3.5E-06	7.6E-03

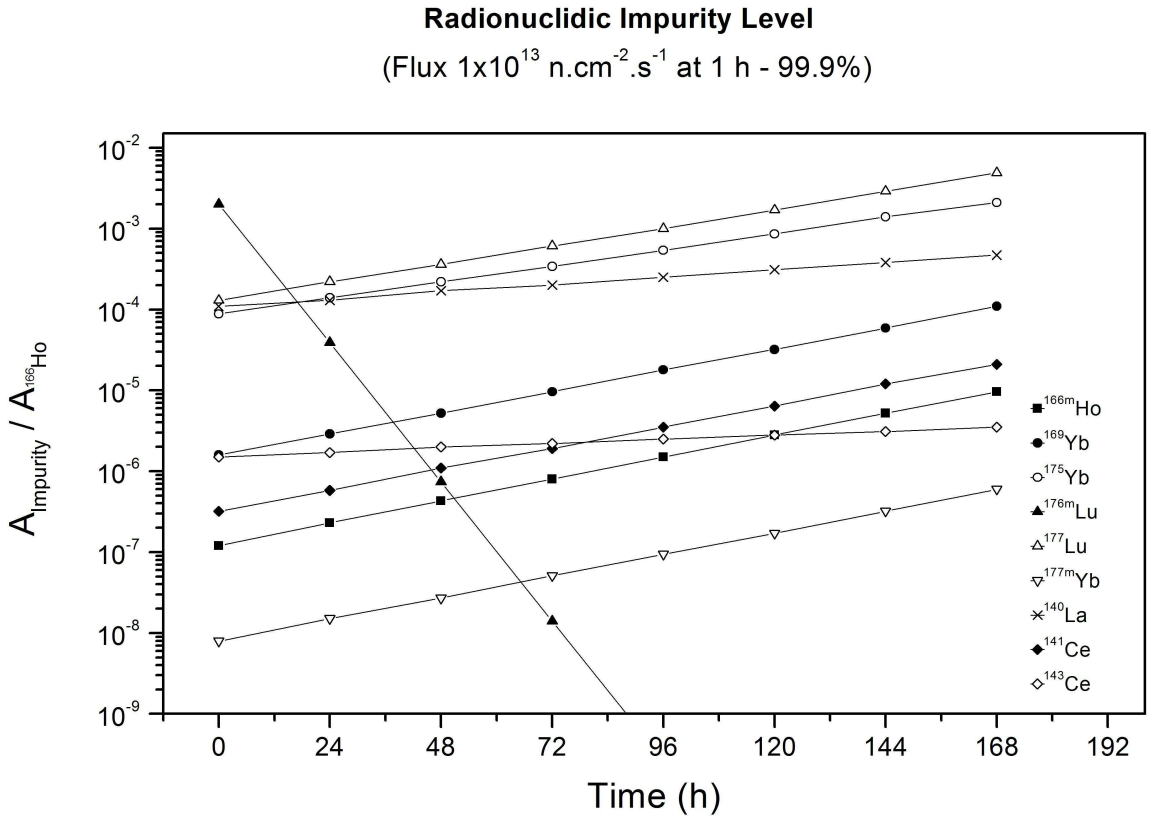

Figure 1. Radionuclidic impurities level to preliminary test conditions.

Table 5. Radionuclidic impurities level to IEA-R1's nowadays maximum conditions.

	Radionuclidic Impurity Level (Flux 5x10^{13} n.cm^{-2}.s^{-1} at 64 h with 99.9%)									
ΔT	^{166m}Ho	^{169}Yb	^{175}Yb	^{176m}Lu	^{177}Lu	^{177m}Lu	^{140}La	^{141}Ce	^{143}Ce	Σ
EOB	2.5E-07	3.0E-06	1.5E-04	3.6E-04	2.3E-04	1.6E-08	1.4E-04	6.3E-07	1.7E-06	8.8E-04
24 h	4.7E-07	5.6E-06	2.3E-04	7.0E-06	3.9E-04	2.9E-08	1.7E-04	1.1E-06	1.9E-06	8.0E-04
48 h	8.7E-07	1.0E-05	3.6E-04	1.3E-07	6.5E-04	5.5E-08	2.1E-04	2.1E-06	2.2E-06	1.2E-03
72 h	1.6E-06	1.9E-05	5.7E-04	2.6E-09	1.1E-03	1.0E-07	2.5E-04	3.8E-06	2.4E-06	1.9E-03
96 h	3.0E-06	3.4E-05	9.0E-04	4.9E-11	1.8E-03	1.9E-07	3.1E-04	6.9E-06	2.8E-06	3.1E-03
120 h	5.6E-06	6.3E-05	1.4E-03	9.4E-13	3.1E-03	3.5E-07	3.8E-04	1.3E-05	3.1E-06	4.9E-03
144 h	1.0E-05	1.2E-04	2.2E-03	1.8E-14	5.1E-03	6.4E-07	4.7E-04	2.3E-05	3.5E-06	8.0E-03
168 h	1.9E-05	2.1E-04	3.5E-03	3.4E-16	8.6E-03	1.2E-06	5.8E-04	4.2E-05	3.9E-06	1.3E-02

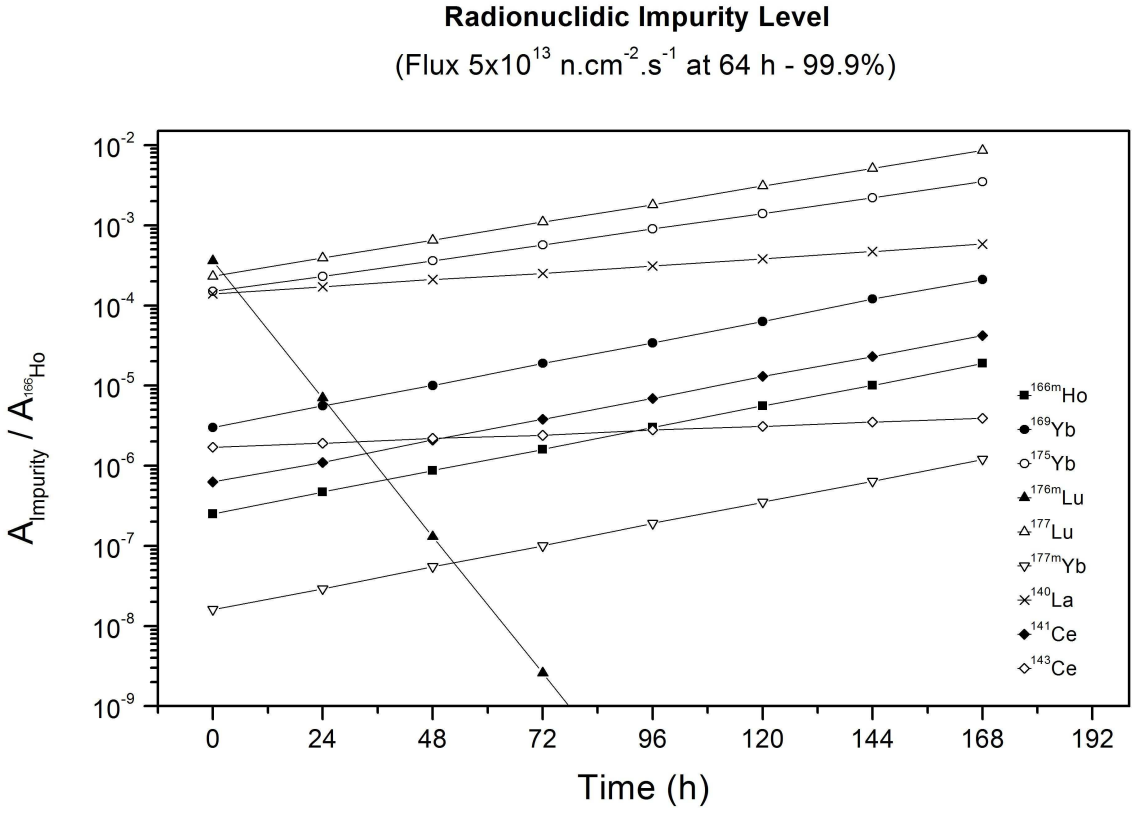

Figure 2. Radionuclidic impurities level to IEA-R1's nowadays maximum conditions.

Table 6. Radionuclidic impurities level to IEA-R1's higher time use conditions.

Radionuclidic Impurity Level (Flux 5x10^{13} n.cm^{-2}.s^{-1} at 120 h with 99.9%)										
ΔT	^{166m}Ho	^{169}Yb	^{175}Yb	^{176m}Lu	^{177}Lu	^{177m}Lu	^{140}La	^{141}Ce	^{143}Ce	Σ
EOB	4.0E-07	4.7E-06	1.9E-04	3.1E-04	3.3E-04	2.5E-08	1.5E-04	9.7E-07	1.8E-06	9.9E-04
24 h	7.4E-07	8.7E-06	3.1E-04	5.9E-06	5.5E-04	4.7E-08	1.9E-04	1.8E-06	2.1E-06	1.1E-03
48 h	1.4E-06	1.6E-05	4.8E-04	1.1E-07	9.2E-04	8.6E-08	2.3E-04	3.2E-06	2.3E-06	1.7E-03
72 h	2.6E-06	2.9E-05	7.6E-04	2.2E-09	1.6E-03	1.6E-07	2.8E-04	5.9E-06	2.6E-06	2.6E-03
96 h	4.8E-06	5.3E-05	1.2E-03	4.2E-11	2.6E-03	3.0E-07	3.5E-04	1.1E-05	2.9E-06	4.2E-03
120 h	8.9E-06	9.8E-05	1.9E-03	8.0E-13	4.4E-03	5.5E-07	4.3E-04	2.0E-05	3.3E-06	6.8E-03
144 h	1.7E-05	1.8E-04	3.0E-03	1.5E-14	7.3E-03	1.0E-06	5.2E-04	3.6E-05	3.7E-06	1.1E-02
168 h	3.1E-05	3.3E-04	4.7E-03	2.9E-16	1.2E-02	1.9E-06	6.5E-04	6.5E-05	4.1E-06	1.8E-02

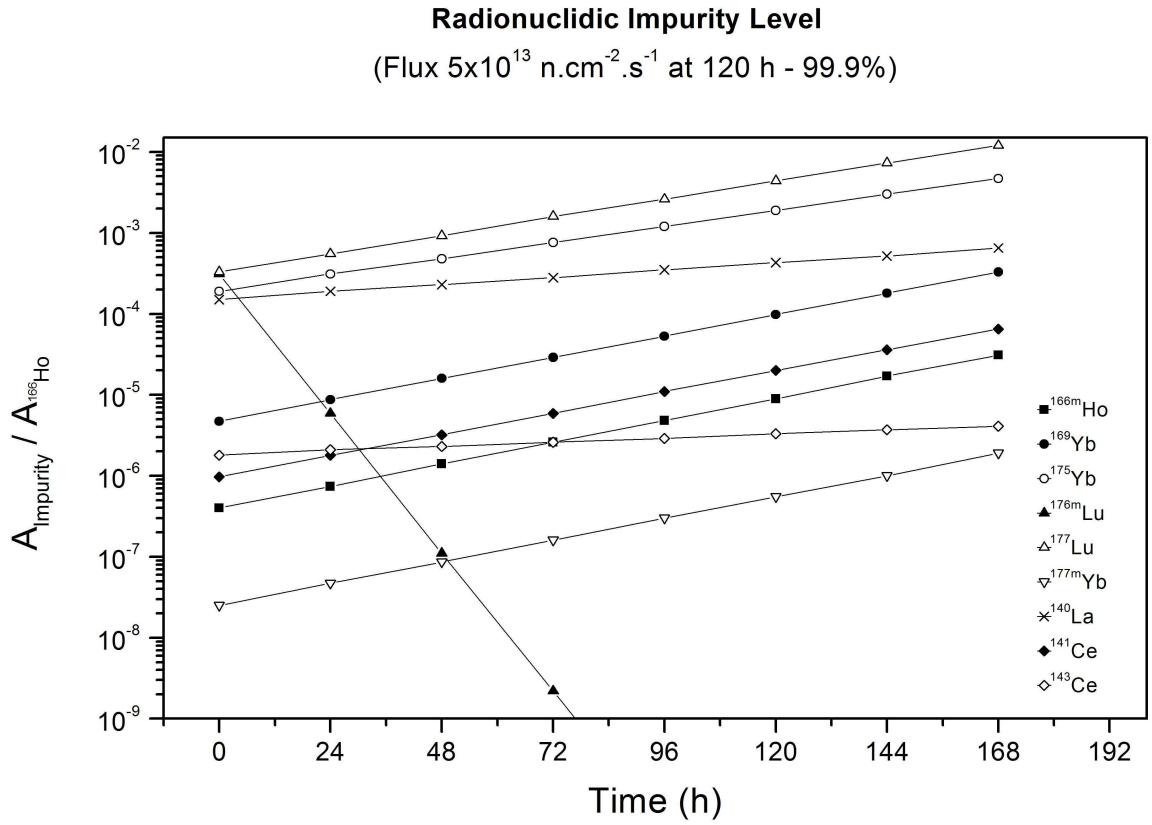

Figure 3. Radionuclidic impurities level to IEA-R1's higher time use conditions.

The relative radionuclidic impurities are altered when different activation times, neutron flux and decay time are applied. This occurs due the different physical properties as cross-section and decay constant. The increase in activation parameters and decay process produces an increased level of total contaminants. However, only the impurity level of ^{176m}Lu decrease quickly after EOB due to its half-life. Considering contamination level by each rare earth of 0.1% and 7 days after EOB the maximum of radionuclidic impurities would be in 7.6x10^{-3}, 1.3x10^{-2} and 1.8x10^{-2}.

The greatest influence on radionuclidic impurity is due to Lutetium with ^{177}Lu production and Ytterbium with ^{175}Yb. In contrast, a lower influence impurity by ^{166m}Ho could be observed. This fact is important because the ^{166m}Ho production is intrinsic to the ^{165}Ho activation process.

3.2. Experimental analyses

The activities have been measured for two kinds of samples, Holmium Oxide and microspheres loaded with holmium. This irradiations process was the preliminary tests with lower conditions. The specific activities results are shown in table 7.

Table 7. Specific activities results by experimental method.

	Experimental - Radionuclides Activity at EOB (Bq.g^{-1})									
Sample	**^{166}Ho**	**^{166m}Ho**	**^{169}Yb**	**^{175}Yb**	**^{176m}Lu**	**^{177}Lu**	**^{177m}Lu**	**^{140}La**	**^{141}Ce**	**^{143}Ce**
Ho_2O_3	25.8E+9	3.5E+3	n/d	n/d	n/d	24.3E+3	n/d	n/d	n/d	n/d
Microspheres	14.3E+9	1.8E+3	27.9E+3	2.3E+6	n/d	480.5E+3	n/d	n/d	n/d	n/d

$^{n/d}$ – Not detected.

These activity results were expected considering the chemical composition of samples with high purity for the holmium oxide and unknown purity of the holmium compound used at the microspheres. The specific activities are used to determine the radionuclidic impurity level for the samples and calculate the percentage of mass contaminants. The impurity levels were established for only one activation condition from the EOB to the maximum decay time of 7 days and results shown in tables 8 and 9 and figures 4 and 5.

Table 8. Radionuclidic impurities level of Holmium Oxide.

	Radionuclidic Impurity Level (Flux 1x10^{13} n.cm^{-2}.s^{-1} at 1 h - Ho_2O_3)									
ΔT	**^{166m}Ho**	**^{169}Yb**	**^{175}Yb**	**^{176m}Lu**	**^{177}Lu**	**^{177m}Lu**	**^{140}La**	**^{141}Ce**	**^{143}Ce**	**Σ**
EOB	1.3E-07	n/d	n/d	n/d	9.4E-07	n/d	n/d	n/d	n/d	1.1E-06
24 h	2.5E-07	n/d	n/d	n/d	1.6E-06	n/d	n/d	n/d	n/d	1.8E-06
48 h	4.6E-07	n/d	n/d	n/d	2.6E-06	n/d	n/d	n/d	n/d	3.1E-06
72 h	8.6E-07	n/d	n/d	n/d	4.4E-06	n/d	n/d	n/d	n/d	5.3E-06
96 h	1.6E-06	n/d	n/d	n/d	7.5E-06	n/d	n/d	n/d	n/d	9.1E-06
120 h	3.0E-06	n/d	n/d	n/d	1.3E-05	n/d	n/d	n/d	n/d	1.5E-05
144 h	5.6E-06	n/d	n/d	n/d	2.1E-05	n/d	n/d	n/d	n/d	2.7E-05
168 h	1.0E-05	n/d	n/d	n/d	3.5E-05	n/d	n/d	n/d	n/d	4.6E-05

$^{n/d}$ – Not detected.

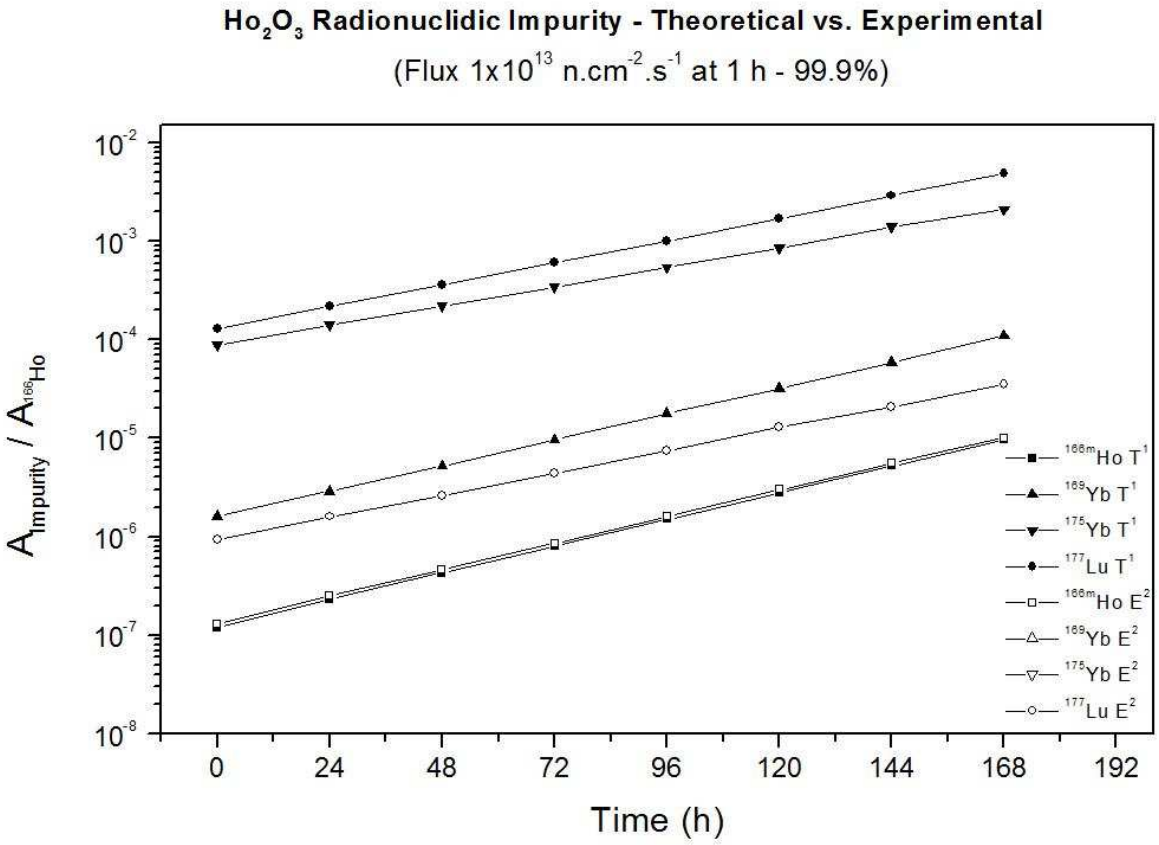

[1] Theoretical method. – [2] Experimental method.

Figure 4. Radionuclidic impurities level of Holmium Oxide.

In holmium oxide samples, two radionuclidic impurities were identified: ^{177}Lu, in higher level and ^{166m}Ho, in lower. After determining the activities and impurities level was evaluated the comparative mass to rare earth impurities by Holmium with 0.0007% to Lutetium.

Table 9. Radionuclidic impurities level of microspheres loaded with Holmium.

	Radionuclidic Impurity Level (Flux 1x10^{13} n.cm^{-2}.s^{-1} at 1 h - Microspheres)									
ΔT	^{166m}Ho	^{169}Yb	^{175}Yb	^{176m}Lu	^{177}Lu	^{177m}Lu	^{140}La	^{141}Ce	^{143}Ce	Σ
EOB	1.3E-07	2.0E-06	1.6E-04	n/d	3.4E-05	n/d	n/d	n/d	n/d	1.9E-04
24 h	2.5E-07	3.6E-06	2.5E-04	n/d	5.7E-05	n/d	n/d	n/d	n/d	3.1E-04
48 h	4.6E-07	6.6E-06	3.9E-04	n/d	9.5E-05	n/d	n/d	n/d	n/d	4.9E-04
72 h	8.6E-07	1.2E-05	6.2E-04	n/d	1.6E-04	n/d	n/d	n/d	n/d	7.9E-04
96 h	1.6E-06	2.2E-05	9.7E-04	n/d	2.7E-04	n/d	n/d	n/d	n/d	1.3E-03
120 h	3.0E-06	4.0E-05	1.5E-03	n/d	4.5E-04	n/d	n/d	n/d	n/d	2.0E-03
144 h	5.5E-06	7.4E-05	2.4E-03	n/d	7.5E-04	n/d	n/d	n/d	n/d	3.3E-03
168 h	1.0E-05	1.4E-04	3.8E-03	n/d	1.3E-03	n/d	n/d	n/d	n/d	5.2E-03

[n/d] – Not detected.

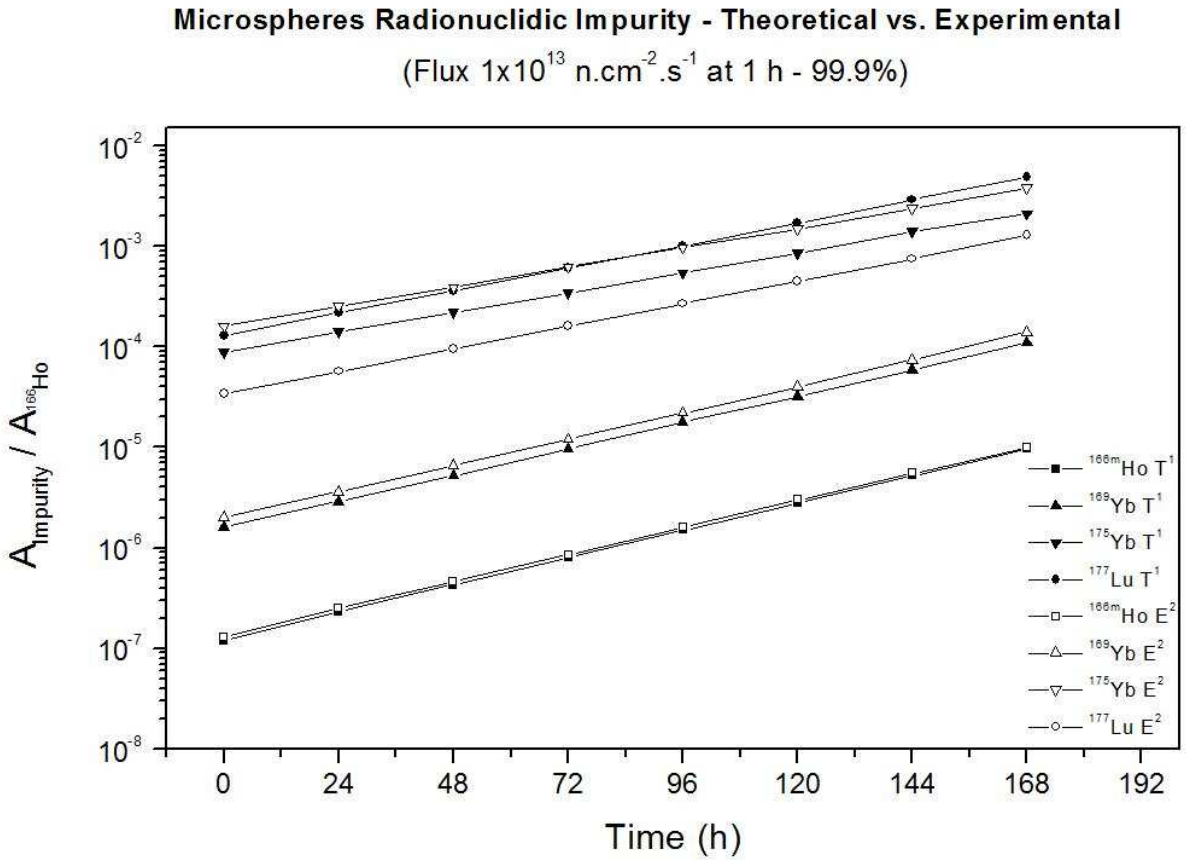

[1] Theoretical method. – [2] Experimental method.

Figure 5. Radionuclidic impurities level of microspheres loaded with Holmium.

Four radionuclidic impurities were identified in microsphere samples. The higher radionuclidic impurity level is ^{175}Yb followed by ^{177}Lu, ^{169}Yb and lower ^{166m}Ho. After determining the activities and impurities level was evaluated the comparative mass to rare earth impurities by Holmium with 0.1529% to Ytterbium and 0.0259% to Lutetium. Both the Holmium Oxide and microspheres found good agreement between theoretical and experimental values to ^{166m}Ho radionuclidic impurity. This occurs because the ^{166m}Ho is intrinsic product of ^{165}Ho activation. However, the others impurities have a high mass dependence.

3. CONCLUSIONS

The aim of this study was to develop a method to determine the possible radionuclidic impurities level of rare earths at microspheres loaded with Holmium. This allows to establish the minimum rare earth purity level required of the chemical Holmium compounds for determine the radionuclidic impurity level.

The present study has demonstrated that good agreement between theoretical and experimental methods to determine de radionuclidic impurities level when material information and activation conditions are well known. Therefore, can be preliminary evaluated any possible radionuclidic impurity originated by contaminants level in the sample before activation process.

These impurities increase the patient dose without providing any benefits and this study allows indicating the optimal time for administration after activation process.

The conditions during neutron activation of the microspheres need to be strictly defined with adjustment of irradiation parameters. This is important to establish the impurities level.

Future studies about the structural integrity of the microspheres and their stability with respect to ^{166}Ho release are still needed.

ACKNOWLEDGMENTS

The authors wish to acknowledge the Comissão Nacional de Energia Nuclear (CNEN) and Instituto de Pesquisas Energéticas e Nucleares (IPEN/CNEN-SP) for granting a fellowship for this project.

REFERENCES

1. "Câncer de fígado", INCA – Instituto Nacional do Câncer http://www.inca.gov.br/conteudo_view.asp?id=330 (2011)
2. Cady, B., "Natural history of primary and secondary tumors of the liver", *Seminary of Oncology*, **Vol. 10,** pp.127-134 (1983).
3. Glenn, S. Jr., Ravikumar, T. S., "Resection of Hepatic Metastases from Colorectal Cancer", *Annals of Surgery*, **Vol. 210,** No. 2, (1989).
4. "Incidência de câncer no Brasil – Estimativa 2010", INCA – Instituto Nacional do Câncer http://www.inca.gov.br/estimativa/2010/ (2011)
5. Anderson, J. H., Angerson, W. J., Willmott, N., Kerr, D. J., McArdle, C. S., Cooke, T. G., "Regional delivery of microspheres to liver metastases: the effects of particle size and concentration on intrahepatic distribution", *Br J Cancer*, **Vol. 64,** pp.1031-1034 (1991).

6. Petriev, V. M., Skvortsov, V. G., Smakhtin, L. A., Ryzhikova, T. P., "Neutron Activation Preparation of 166Ho-Albumin Microspheres as a Promising Radiopharmaceutical for Tumor Therapy", *Radiochemistry*, **Vol. 47,** No. 3, pp.301-314 (2005).
7. Squair, P. L.; Pozzo, L.; Ivanov, E.; Azevedo, M. B. M.; Souza, J. R.; Pires, G.; Nascimento, N.; Osso, J. A., "Neutron activation of microspheres containing 165Ho: preliminary results", *18th International Conference on Medical Physics: Science and Technology for Health for All - ICMP 2011*, Code 442**,** PO1-NM-20, draft, April 17-20, Porto Alegre, Brazil (2011).
8. Mumper R. J., Ryo U. Y., Jay M., "Neutron activated holmium-166-poly (L-lactic acid) microspheres: a potential agent for the internal radiation therapy of hepatic tumours", *Nuclear Medicine*, **Vol. 32,** pp.2139-2143 (1991).
9. Turner J. H., Claringbold P. G., Klemp P. F. B., Cameron P. J., Martindale A. A., Glancy R. J., Norman P. E., Hetherington E. L., Najdovski L., Lambrecht R. M., "166Ho-microsphere liver radiotherapy: a preclinical SPECT dosimetry study in the pig", *Nuclear Medicine Comun*, **Vol. 15,** pp.545-553 (1994).
10. Bardiès, M., Chatal, J., "Absorbed doses for internal radiotherapy from 22 beta-emitting radionuclides: beta dosimetry of small spheres", *Physical Medicine Biology*, **Vol. 39,** pp.961-981 (1994).
11. Nguyen, V. D., Pham, D. K., Kim, G., et.al. , "Measurement of thermal neutron cross-section and resonance integral for the ^{165}Ho(n,c)^{166g}Ho reaction using electron linac-based neutron source", *Nuclear Instruments and Methods in Physics Research*, **Vol. 269,** pp.159-166 (2010).
12. IAEA – International Atomic Energy Agency., "Manual for reactor produced radioisotopes", *IAEA-TECDOC-1340*, Vienna, Austria (2003).
13. Nijsen J.F.W., Zonnenberg B.A., Woittiez J.R.W., Rook D.W., Swildens-van Woudenberg I.A., Van Rijk P.P., van het Schip A.D., "Holmium-166 poly lactic acid microspheres applicable for intra-arterial radionuclide therapy of hepatic malignancies: effects of preparation and neutron activation techniques", *European Journal of Nuclear Medicine*, **Vol. 26, Nº7,** pp.699-704 (1999).
14. "Table of Radioactive Isotopes, Nuclide Search – WWW Table of Radioactive Isotopes, ENSDF citation", Ernest Orlando Lawrence, Berkeley National Laboratory, http://nucleardata.nuclear.lu.se/nucleardata/toi/radSearch.asp (2011).